Supporting Information

Unravelling the origin of dual photoluminescence in Au_2Cu_6 clusters by triplet sensitization and photon upconversion

Daichi Arima, Yoshiki Niihori, Masaaki Mitsui*

Department of Chemistry, College of Science, Rikkyo University, 3-34-1, Nishiikebukuro, Toshima-ku, Tokyo, 171-8501, Japan.

Corresponding author

*E-mail: mitsui@rikkyo.ac.jp

Contents

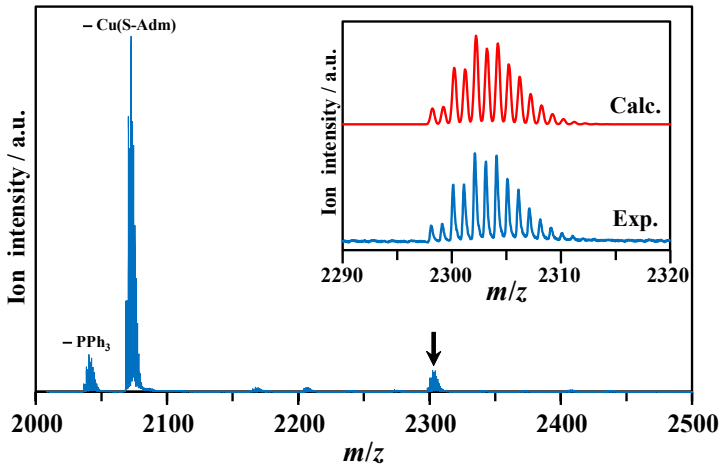

Fig. S1. Positive-ion mode ESI-mass spectrum of $Au_2Cu_6(S\text{-}Adm)_6(PPh_3)_2$. The daughter ions of Cu(S-Adm) or PPh_3 dissociated from the parent ion were also observed.

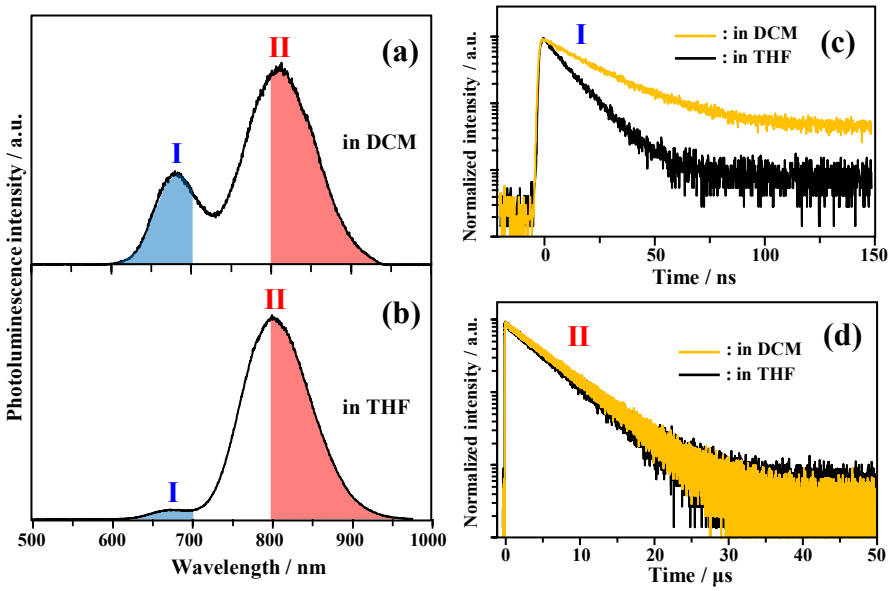

Fig. S2 PL spectra of $Au_2Cu_6(S\text{-}Adm)_6(PPh_3)_2$ (10 μM) in a) DCM and b) THF. To perform band-separated PL lifetime measurements, photons with wavelengths in the filled regions, c) $\lambda \leq 700$ nm of band-I or d) $\lambda \geq 800$ nm of band-II, were selectively recorded using appropriate filters. As a result, only the fast or slow decay component is observed for band-I or -II, respectively.

Evaluation of photoluminescence quantum yield by relative method

The relative PL quantum yield (Φ_{PL}) was calculated using the following equation:

$$\Phi_{PL} = \frac{I_r\left(1 - 10^{-A_r(\lambda_{ex})}\right)\int F_s(\lambda_{em})d\lambda_{em} {n_s}^2}{I_s\left(1 - 10^{-A_s(\lambda_{ex})}\right)\int F_r(\lambda_{em})d\lambda_{em} {n_r}^2}\Phi_f^r, \qquad \text{(S1)}$$

where Φ_f^r represents the known fluorescence quantum yield of the reference dye, A, F, and I represent the absorbance at the excitation wavelength (λ_{ex}), the PL intensity, and excitation laser intensity, respectively, and n is the refractive index of the corresponding solvent. PDI (Φ_f = 0.97 in toluene)[1] was used as a standard for 532 nm excitation.

Photostability of Au_2Cu_6 in DCM and THF

The dynamic light scattering apparatus (nanoSAQLA, Otsuka electronics Co., Ltd.) was used to evaluate the average particle size in solution, as depicted in Fig. S3. When the DCM solution of the $Au_2Cu_6(S\text{-}Adm)_6(PPh_3)_2$ clusters was exposed to room light for 1 hour, the formation of nanoparticles with an average diameter of ca. 40 nm was observed, as shown in the right panel of Fig. S3c. The results suggest that light irradiation induces dissociation of the organic ligands from the clusters, leading to the aggregation of the metal atoms.

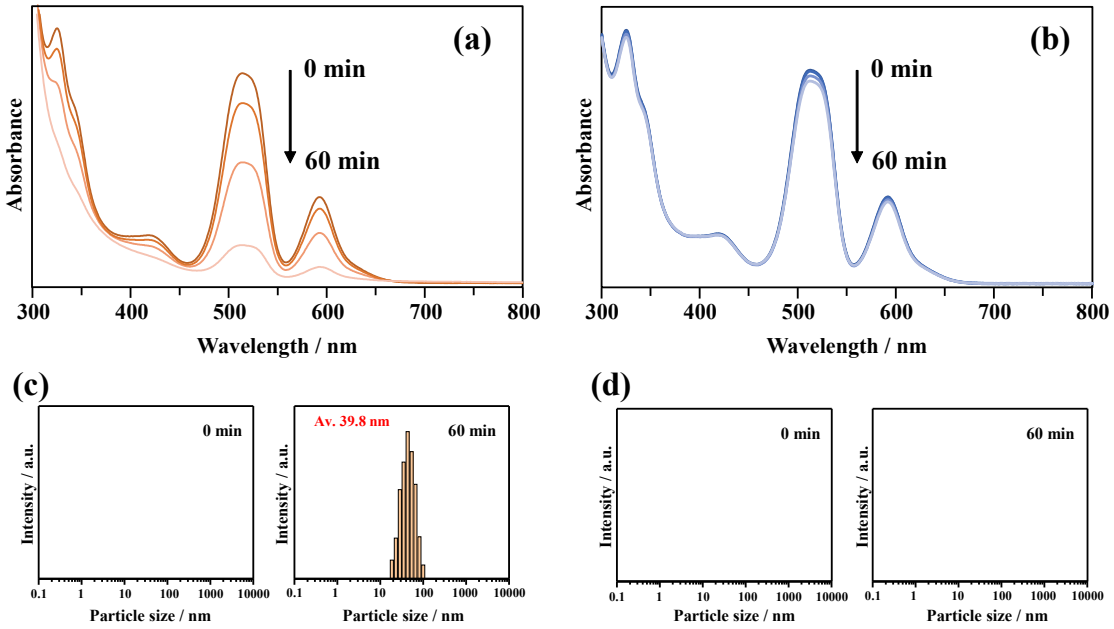

Fig. S3 Time evolution of absorption spectra and particle size distribution, obtained using dynamic light scattering measurements, of $Au_2Cu_6(S\text{-}Adm)_6(PPh_3)_2$ in aerated (a,c) DCM and (b,d) THF solutions under room light.

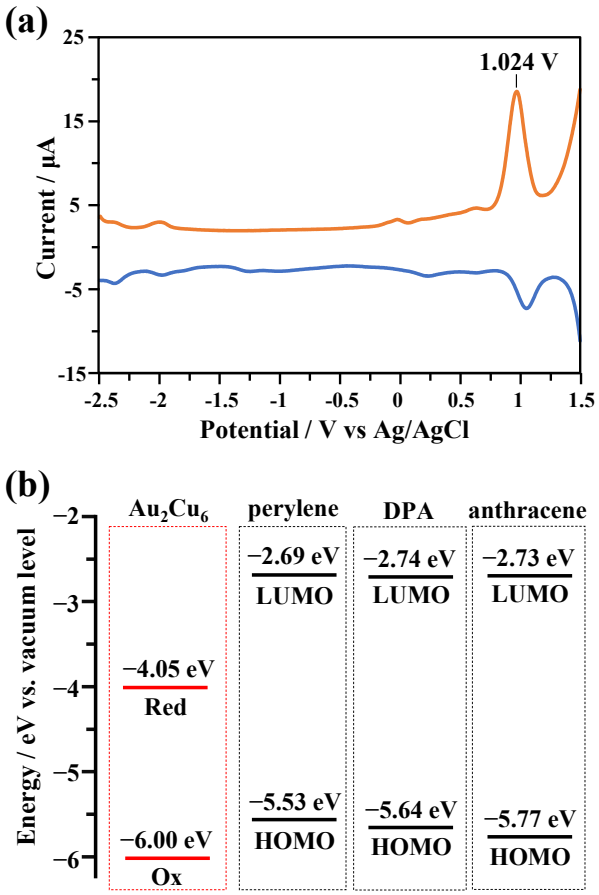

Fig. S4 a) Differential pulse voltammetry signals of $Au_2Cu_6(S\text{-}Adm)_6(PPh_3)_2$ (10 μM) in acetonitrile and b) redox potentials of $Au_2Cu_6(S\text{-}Adm)_6(PPh_3)_2$, perylene, DPA, and anthracene.

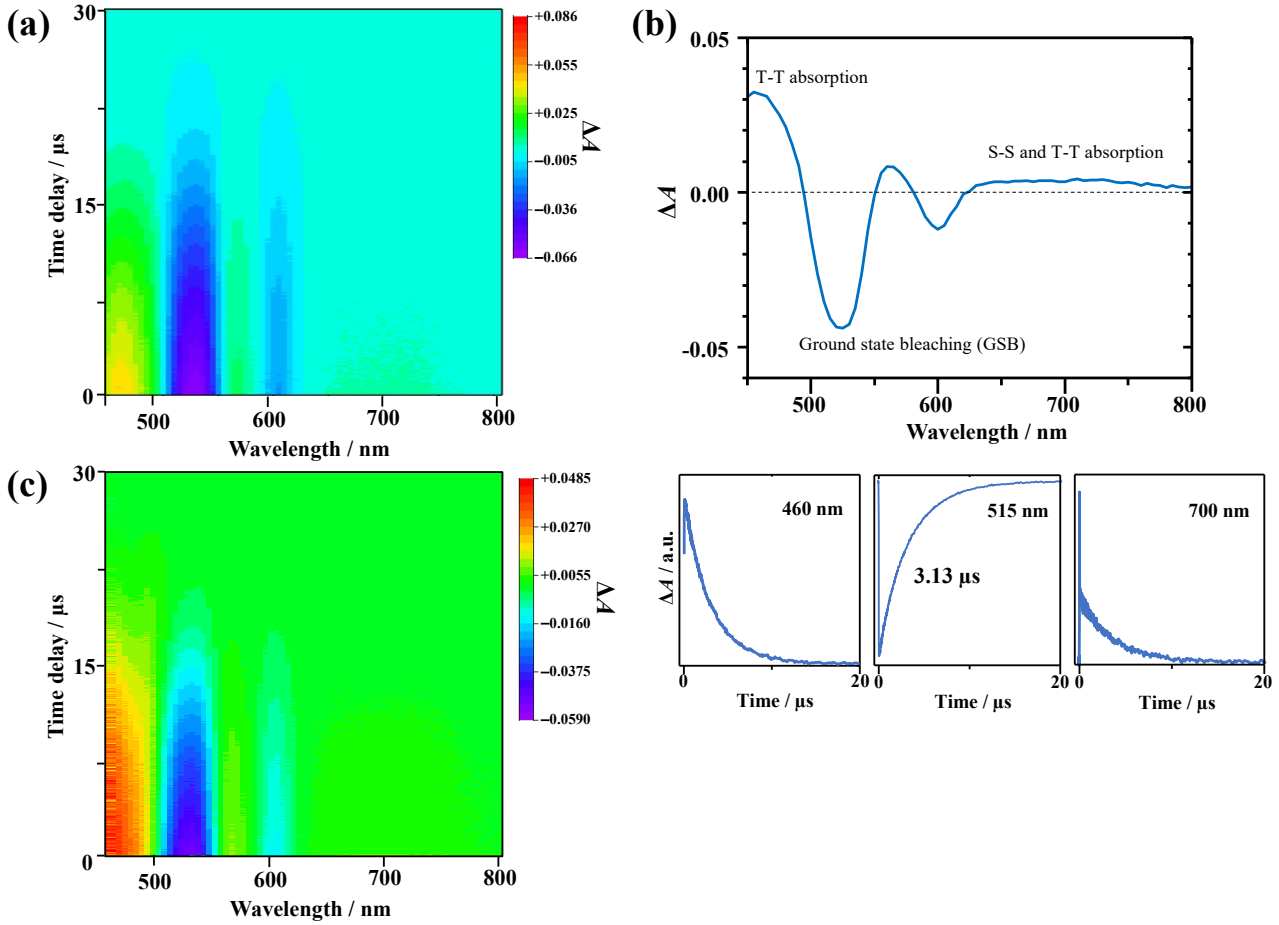

Fig. S5 Transient absorption (TA) spectra which show ΔA from 0 to 30 μs time delays of Au_2Cu_6(S-Adm)$_6$(PPh_3)$_2$ (270 μM) in deaerated THF with excitation at 532 nm. b) Transient absorption spectrum at 1 μs time delay and corresponding time profiles at 460, 515, and 700 nm. c) TA spectra obtained for Au_2Cu_6(S-Adm)$_6$(PPh_3)$_2$ (270 μM) with perylene (10 mM) in deaerated THF with excitation at 532 nm.

Triplet energy transfer (TET) efficiency

The TET efficiency (Φ_{TET}) can be estimated by performing quenching measurements of the PL lifetimes of the sensitizer, as described by the Stern-Volmer relationship as follows:

$$\frac{\tau_0}{\tau} = 1 + K_{SV}[E] \qquad (S2)$$

where K_{SV} is the Stern−Volmer constant, [E] is the emitter concentration, and τ_0 and τ correspond to the unquenched and quenched PL lifetimes of the sensitizer, respectively. In the present case, τ_0 corresponds to the phosphorescence lifetime (τ_p) of Au_2Cu_6(S-Adm)$_6$(PPh_3)$_2$. The Φ_{TET} was calculated by the following equation:

$$\Phi_{TET} = \frac{K_{SV}[E]}{1 + K_{SV}[E]} = \frac{k_{TET}\tau_0[E]}{1 + k_{TET}\tau_0[E]} \qquad (S3)$$

The results are summarized in Table S1.

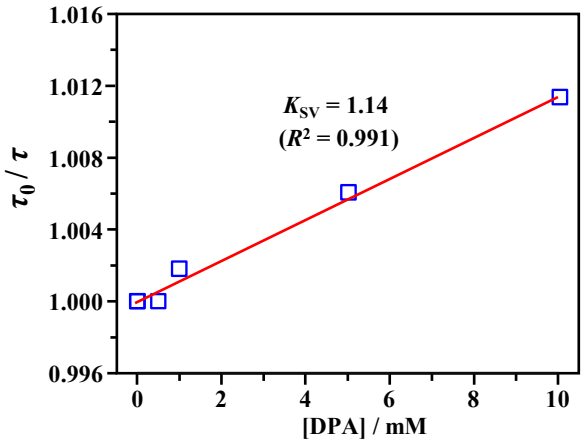

Fig. S6. Stern−Volmer plots of PL quenching of $Au_2Cu_6(S\text{-}Adm)_6(PPh_3)_2$ by DPA emitter (λ_{ex} = 532 nm).

Table S1. **Estimated rate constants for triplet energy transfer (TET) from the Au_2Cu_6 cluster sensitizers to emitters (λ_{ex} = 640 nm).**

Sensitizer	Emitter	E_T / eV	K_{SV} / M^{-1}	k_{TET} / $M^{-1}s^{-1}$	Φ_{TET}
$Au_2Cu_6(S\text{-}Adm)_6(PPh_3)_2$	perylene	1.53	93.9	1.91×10^7	0.32[a]
	DPA	1.77	1.14	2.32×10^5	0.022[b]
	anthracene	1.84	-		-

[a] At 5 mM of perylene. [b] At 20 mM of DPA.

Emitter quenching yield Φ_q and optical outcoupling yield Φ_{out}

The details of how to evaluate Φ_{out} and Φ_q have already been reported in ref. 2, and will be briefly described here. In order to obtain the value of Φ_q, the emitter triplet lifetime (τ_T) for each sensitizer concentration was determined by fitting the UC emission decay curve, $I(t)$, using the following equation:[3]

$$I(t) = I(0)\left(\frac{1-\beta}{\exp\left(t/\tau_T\right) - \beta}\right)^2 \qquad (S4)$$

where

$$\beta = \frac{2k_{TTA}\left[{}^3E^*\right]_0}{1/\tau_T + 2k_{TTA}\left[{}^3E^*\right]_0} \quad (0 < \beta < 1). \qquad (S5)$$

Fig. S7a shows the TF-UC emission decay curves obtained at different cluster sensitizer concentrations and the extracted values of τ_T and β are summarized in Table S2.

As shown in Fig. S7b, the values of τ_T were plotted against $[Au_2Cu_6]$ to generate Stern–Volmer plots described by the following relationship:

$$\frac{1}{\tau_T} = \frac{1}{\tau_{T0}} + k_q[Au_2Cu_6]. \qquad (S6)$$

Additionally, the quenching efficiency (Φ_q) is calculated by

$$\Phi_q = \frac{k_q\tau_{T0}[Au_2Cu_6]}{1 + k_q\tau_{T0}[Au_2Cu_6]}. \qquad (S7)$$

The results are summarized in Table S3.

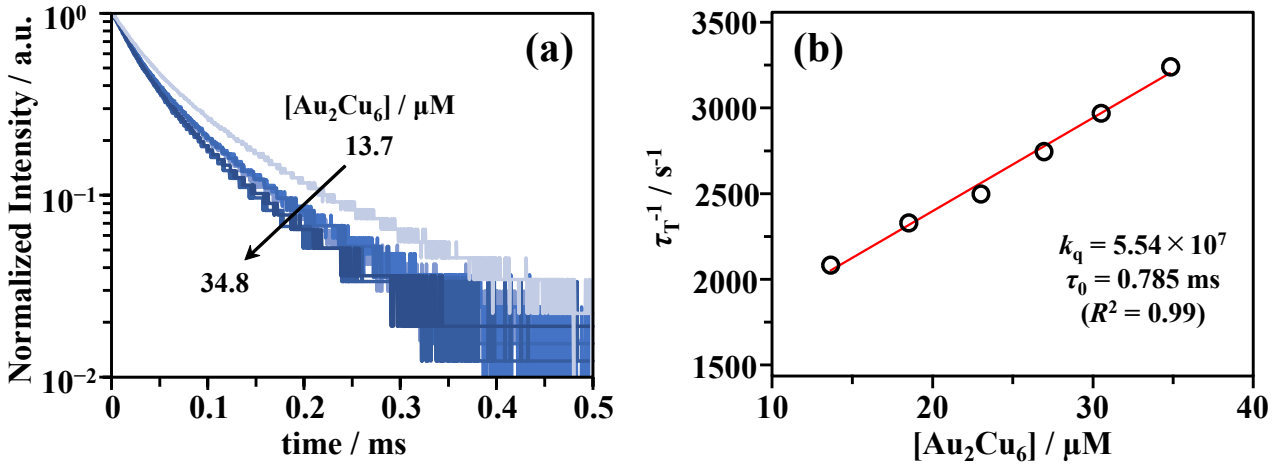

Fig. S7 (a) Triplet fusion upconversion (TF-UC) emission decay curves of solutions containing different concentrations of $Au_2Cu_6(S\text{-}Adm)_6(PPh_3)_2$ with 5.0 mM perylene excited at 532 nm with excitation intensity of 7.9 Wcm^{-2}.

Table S2. Triplet lifetimes of perylene in deaerated THF containing different Au_2Cu_6 sensitizer concentrations.

$[Au_2Cu_6]$ / μM	τ_T / ms	β
13.7	0.48	0.83
18.4	0.43	0.85
23.2	0.40	0.84
26.9	0.37	0.82
30.4	0.34	0.83
34.8	0.31	0.81

Table S3. Emitter triplet lifetime in the absence of sensitizer (τ_{T0}) and quenching rate constant (k_q) and quenching efficiency (Φ_q) of triplet emitter by sensitizer.

sensitizer	emitter	τ_{T0} / μs	k_q / $M^{-1}s^{-1}$	$k_q[Au_2Cu_6]$ / s^{-1} [a]	Φ_q [a]
Au_2Cu_6	perylene	785	5.54×10^7	6.86×10^2	0.35

[a] $[Au_2Cu_6]$ = 12.4 μM.

For Φ_{out}, it can be obtained from the following equation:

$$\Phi_{out} = \frac{\int F_0(\lambda) \cdot 10^{-\frac{A(\lambda)}{2}} d\lambda}{\int F_0(\lambda) d\lambda}. \qquad (S8)$$

where $F_0(\lambda)$ is the emission intensity at a wavelength λ in a dilute solution. The absorbance at a wavelength λ of the UC solution, $A(\lambda)$, was measured under an optical path length of 1.0 cm. In the PL measurement, the excitation light focused on the center of the 1.0 × 1.0 cm cuvette, so the optical path length of the emitted UC photons is 0.5 cm, and the actual observed emission intensity can be expressed as $F_0(\lambda) \cdot 10^{-A(\lambda)/2}$.

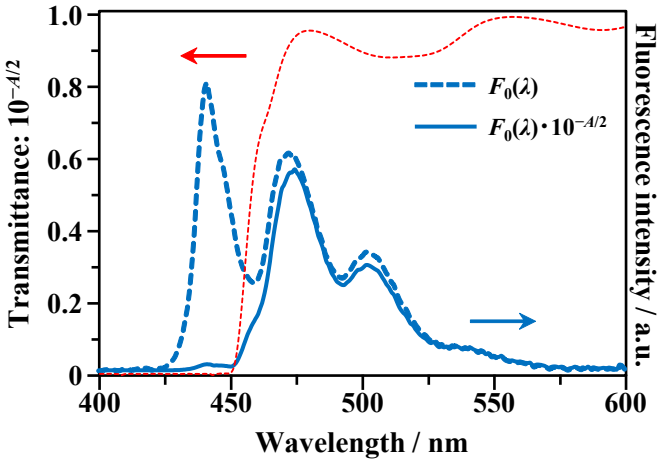

Fig. S8. Fluorescence spectrum (dashed line) of perylene (1 μM) in THF (λ_{ex} = 405 nm) and transmittance curve (dotted line), given by $10^{-A(\lambda)/2}$, of a mixed solution containing 12.4 μM Au_2Cu_6 and 5 mM perylene. The corrected fluorescence spectrum (solid line) obtained by multiplying the fluorescence spectrum of perylene in dilute solution by the transmittance curve is in good agreement with the measured UC spectrum (Fig. 4a).

Temperature dependence of photoluminescence

The temperature dependence of the PL of the $Au_2Cu_6(S\text{-}Adm)_6(PPh_3)_2$ cluster in deaerated THF was measured using a variable temperature cell holder (CoolSpeK, Unisoku Co., Ltd.). The results obtained are shown in Table S4 and S5.

Table S4. Temperature dependence of emission maximum wavelengths (λ_f, λ_p), lifetimes (τ_f, τ_p), and quantum yields (Φ_f, Φ_p) of fluorescence and phosphorescence, together with corresponding PL, ISC, and IC quantum yields of $Au_2Cu_6(S\text{-}Adm)_6(PPh_3)_2$ clusters in deaerated THF.

T / K	λ_f / nm	τ_f / ns	λ_p / nm	τ_p / μs	Φ_f [a]	Φ_{PL}	Φ_p [a]	Φ_{ISC}	Φ_{IC}	Φ_{ISC}' [b]
293	677	9.0	802	4.91	0.0051	0.21	0.44	0.47	0.52	0.56
273	680	13	805	5.35	0.0074	0.18	0.51	0.35	0.64	0.49
253	679	23	807	5.66	0.013	0.17	0.54	0.30	0.68	0.46
233	677	86	811	6.19	0.049	0.12	0.59	0.20	0.75	0.41
213	675	124	813	6.79	0.071	0.077	0.65	0.12	0.81	0.35
193	675	352	814	7.69	0.20	0.062	0.74	0.084	0.71	0.26
173	677	1540	814	8.83	0.88	0.059	0.85	0.069	0.051	0.15

[a] Fluorescence and phosphorescence quantum yields at 173-273 K were estimated using $k_f\tau_f$ and $k_p\tau_p$, respectively. The radiative rate constants were assumed to be temperature-independent, and $k_f = 5.7 \times 10^5$ and $k_p = 9.0 \times 10^4$ s^{-1} obtained at 293K were used. [b]Quantum yield and rate constant of ISC from T_1 to S_0.

Table S5. Temperature dependence of singlet and triplet radiative rate constants (k_f and k_p), rate constants of S_1-T_1 and T_1-S_0 intersystem crossing (k_{ISC} and k_{ISC}') and internal conversion of $Au_2Cu_6(S\text{-}Adm)_6(PPh_3)_2$ clusters in deaerated THF.

T / K	k_f / s^{-1}	k_{ISC} / s^{-1}	k_{IC} / s^{-1}	k_p / s^{-1}	k_{ISC}' / s^{-1}
293		5.3×10^7	5.8×10^7		1.1×10^5
273		2.7×10^7	4.9×10^7		9.2×10^4
253		1.3×10^7	3.0×10^7		8.1×10^4
233	5.7×10^5	2.3×10^6	8.8×10^6	9.0×10^4	6.6×10^4
213		9.5×10^5	6.5×10^6		5.2×10^4
193		2.4×10^5	2.0×10^6		3.4×10^4
173		4.5×10^4	3.3×10^4		1.7×10^4

Table S6. S_0-to-S_n (n = 1–5) and S_0-to-T_n (n = 1–3) vertical transition wavelengths (energies), oscillator strengths (f), configuration interactions (CI), and expansion coefficients (P) of Au_2Cu_6 obtained by theoretical calculations.

Excited state	wavelength / nm (eV) [a]	f [b]	Dominant configuration	CI expansion coefficient [c]
T_1	572.82 (2.1645)	0.0000	H → L	0.61526 (97%)
T_2	572.21 (2.1667)	0.0000	H → L+1	0.69822 (97%)
S_1	496.63 (2.4965)	0.1427	H → L	0.68162 (92%)
S_2	496.20 (2.4987)	0.1423	H → L+1	0.68162 (92%)
T_3	449.66 (2.7573)	0.0000	H-1 → L	0.68915 (94%)
S_3	430.63 (2.8791)	0.0721	H → L+2	0.70035 (98%)
S_4	428.41 (2.8940)	0.0034	H-1 → L	0.68266 (93%)
S_5	428.02 (2.8967)	0.0033	H-1 → L+1	0.68265 (93%)

[a]The values in brackets are in eV. [b]Note that S_0-to-T_n transitions have zero oscillator strengths because transitions to excited triplet states are spin forbidden under the present calculations including no spin–orbit coupling effect. [c]The values in brackets are the percentage contribution ($P = 2|CI|^2$).

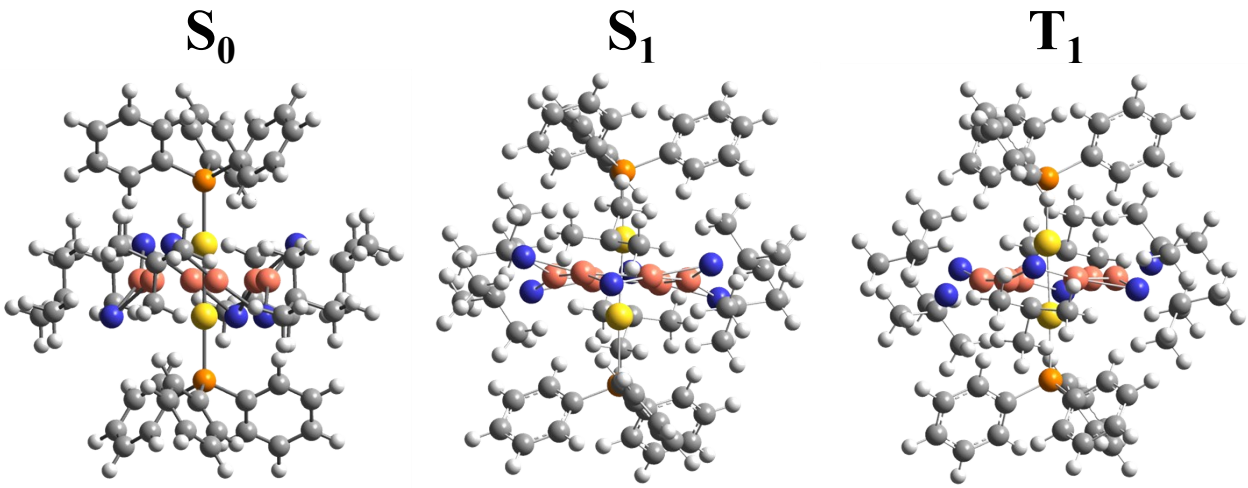

File Type	.log	
Calculation Type	FREQ	
Calculation Method	RBP86	
Basis Set	Gen	
Charge	0	
Spin	Singlet	
Solvation	None	
E(RB-P86)	-6855.435082	Hartree
RMS Gradient Norm	0.000049	Hartree/Bohr
Imaginary Freq	0	
Dipole Moment	0.004423	Debye
Polarizability (α)	1105.732197	a.u.
Point Group	C1	

File Type	.log	
Calculation Type	FREQ	
Calculation Method	RBP86 TD-FC	
Basis Set	Gen	
Charge	0	
Spin	Singlet	
Solvation	None	
E(TD-HF/TD-DFT)	-6855.387584	Hartree
RMS Gradient Norm	0.000014	Hartree/Bohr
Imaginary Freq	0	
Dipole Moment	0.001257	Debye
Polarizability (α)	1511.835960	a.u.
Point Group	C1	

File Type	.log	
Calculation Type	FREQ	
Calculation Method	RBP86 TD-FC	
Basis Set	Gen	
Charge	0	
Spin	Singlet	
Solvation	None	
E(TD-HF/TD-DFT)	-6855.392444	Hartree
RMS Gradient Norm	0.000013	Hartree/Bohr
Imaginary Freq	0	
Dipole Moment	0.003434	Debye
Polarizability (α)	1271.464657	a.u.
Point Group	C1	

Fig. S9 Optimized structures of $Au_2Cu_6(S\text{-}CMe_3)_6(PPh_3)_2$ in the S_0, S_1, and T_1 states (upper panel), together with their Gaussian calculation summary provided using GaussView 6.0 (lower panel).

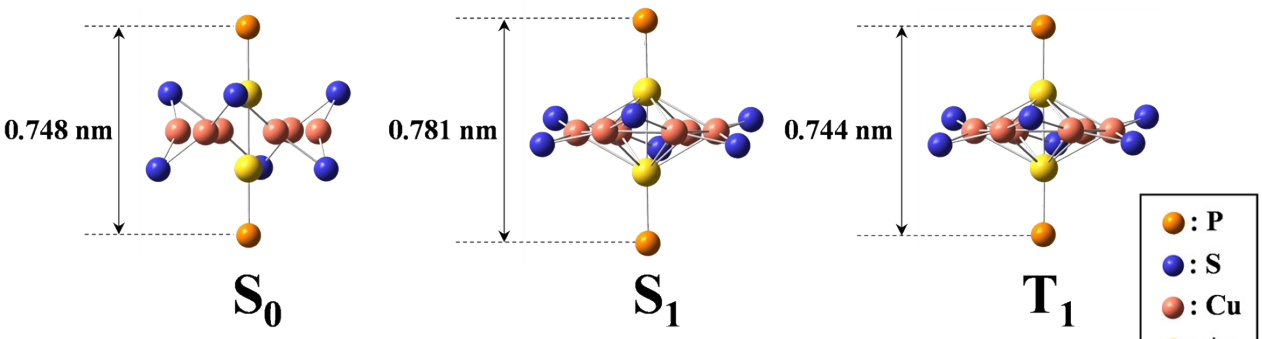

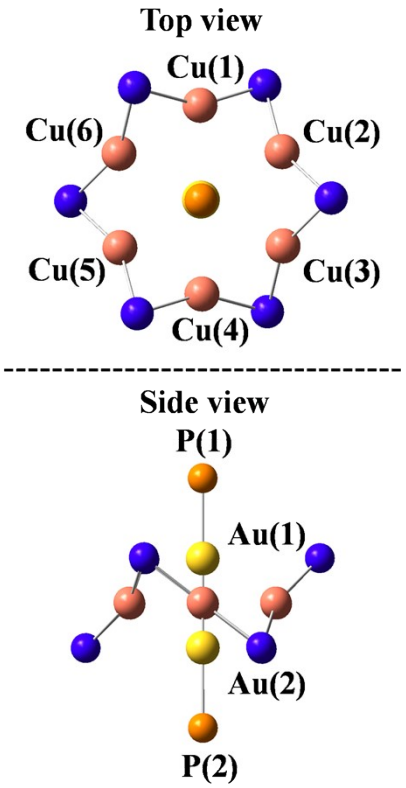

Bond	S_0	S_1	T_1
	Bond length / Å		
P(1)-Au(1)	2.40424	2.49558	2.38361
P(2)-Cu(2)	2.40413	2.49561	2.38359
Au(1)-Au(2)	2.67265	2.82170	2.67285
Cu(1)-Cu(2)	2.53858	2.44960	2.43302
Cu(2)-Cu(3)	2.53855	2.45532	2.57647
Cu(3)-Cu(4)	2.53907	2.46229	2.46238
Cu(4)-Cu(5)	2.53834	2.44959	2.43303
Cu(5)-Cu(6)	2.53803	2.45530	2.57651
Cu(6)-Cu(1)	2.53896	2.46229	2.46239

Fig. S10. Optimized structures of $Au_2Cu_6(S\text{-}CMe_3)_6(PPh_3)_2$ in the S_0, S_1, and T_1 states (upper panel). For clarity, only the Au_2Cu_6 moiety with two P atoms is shown and the ligand parts are excluded; the full structures are given in Fig. S9. The Au-Au bond remains almost unchanged between the S_0 and T_1 states, but is significantly elongated in the S_1 state. The crown structure of the Cu_6S_6 site, which is highly zigzagged in the S_0 state, approaches a much more planar structure in the S_1 and T_1 states. The bond lengths in the S_0, S_1, and T_1 states (bottom panel). The ring structure consisting of six copper atoms is D_{6h}-like regular hexagonal in the S_0 state, but in the S_1 state and especially in the T_1 state, the symmetry is reduced to a distorted hexagon.

References

(1) S. Prathapan, S. I. Yang, J. Seth, M. A. Miller, D. F. Bocian, D. Holten, J. S. Lindsey, *J. Phys. Chem.*, *B* 2001, **105**, 8237.

(2) Y. Niihori, Y. Wada, M. Mitsui, *Angew. Chem. Int. Ed.*, 2021, **60**, 2822.

(3) E. M. Gholizadeh, L. Frazer, R. W. MacQueen, J. K. Gallahera, T. W. Schmidt, *Phys. Chem. Chem. Phys.*, 2018, **20**, 19500.